

# Chemical Science

[rsc.li/chemical-science](https://rsc.li/chemical-science)



ISSN 2041-6539



Cite this: *Chem. Sci.*, 2020, **11**, 4305

All publication charges for this article have been paid for by the Royal Society of Chemistry

Received 26th February 2020  
Accepted 20th March 2020

DOI: 10.1039/d0sc01159b  
[rsc.li/chemical-science](http://rsc.li/chemical-science)

## Introduction

Since Gilbert N. Lewis formulated the two-electron process between an electron-pair acceptor and donor, termed the Lewis acid and base, respectively in 1923,<sup>1</sup> the concept of Lewis pairs has been regarded as one of the most fundamental principles in chemical science. Primarily, the chemistry of Lewis pairs has been understood and developed within a direct two-electron transfer manifold to form a dative-bonded adduct (Lewis acid-base adduct or Lewis adduct). The formation of a coordination bond leads to the activation of both the Lewis acid and base, which has been exploited in various fields of chemistry, especially in synthetic chemistry, exemplified by Lewis acid catalysis involving electrophilic activation of carbonyl compounds for selective bond-forming reactions.<sup>2</sup> Meanwhile, indirect two-electron transfer between Lewis pairs is operative in the arena of frustrated Lewis pairs (FLPs).<sup>3</sup> In this process, Lewis acids and bases can not form a conventional Lewis adduct due to steric congestion, and thus, the resultant encounter complex acquires the capability of activating small molecules, such as dihydrogen, in a cooperative manner. On the other hand, single-electron transfer (SET) from a Lewis base to a Lewis acid to generate, in principle, a pair of a Lewis base-derived radical cation and a Lewis

acid-derived radical anion has been invoked since the 1960s,<sup>4</sup> and recent seminal studies have uncovered that SET is a viable mechanism for the reactions of frustrated and conventional Lewis pairs.<sup>5</sup> However, the operation of this SET mechanism is limited to specific Lewis pairs, and despite its significant potential as a general means for the generation of radical-ion pairs as a reactive species, its utility in organic synthesis and catalysis remains elusive.<sup>6</sup> This is probably due to an insufficient understanding of the possible intermediate and/or transition states of the SET process, particularly in FLPs, while the resulting radical ions have been directly observed and characterized by taking advantage of their stability owing to the steric and electronic nature pertinent to slowing back-electron transfer (BET).

Under these circumstances, we paid our attention to the underlying similarity between FLPs and electron donor-acceptor (EDA) complexes (or charge-transfer (CT) complexes) as precursors of radical-ion pairs,<sup>7</sup> considering that not only  $\pi$ -acceptors and donors but also  $\sigma$ -acceptors such as  $\text{Br}_2$ ,<sup>8</sup>  $\text{I}_2$ ,<sup>9</sup>  $\text{NO}^+$ <sup>10</sup> and hypervalent iodine compounds,<sup>11</sup> and  $\sigma$ -donors such as cyclic alkylamines<sup>11c,12</sup> serve as partners for EDA complexes. Upon complexation, an electron donor and an acceptor are weakly associated without the formation of a coordination bond, within an appropriate distance to realize orbital interactions for undergoing an internal SET, which could be regarded as a form of an encounter complex proposed in FLP chemistry.<sup>13</sup> We envisaged that this interpretation of the mode of molecular association in the encounter complex could provide a clue for the understanding and generalization of the SET in Lewis pairs, which would be beneficial for its broad exploitation, specifically in the development of one-electron-mediated catalysis relevant to organic synthesis. Herein, we demonstrate that an SET between a common Lewis acid, tris(pentafluorophenyl)borane ( $\text{B}(\text{C}_6\text{F}_5)_3$ ), and simple *N,N*-dialkylanilines operates through the formation of an EDA complex as a key intermediate under dark

<sup>a</sup>Institute of Transformative Bio-Molecules (WPI-ITbM), Department of Molecular and Macromolecular Chemistry, Graduate School of Engineering, Nagoya University, Nagoya 464-8601, Japan. E-mail: [tooi@chembio.nagoya-u.ac.jp](mailto:tooi@chembio.nagoya-u.ac.jp)

<sup>b</sup>Institute of Materials and Systems for Sustainability, Nagoya University, Nagoya 464-8601, Japan

<sup>c</sup>CREST, Japan Science and Technology Agency (JST), Nagoya University, Nagoya 464-8601, Japan

† Electronic supplementary information (ESI) available: UV-vis absorption, ESR, electrochemical measurement, X-ray crystallography, computational studies, experimental procedures for catalytic reactions and characterization for all relevant compounds. CCDC 1986458. For ESI and crystallographic data in CIF or other electronic format see DOI: 10.1039/d0sc01159b



conditions or visible-light irradiation depending on the structure of the aniline derivative. This inherent SET initiates the generation of the corresponding  $\alpha$ -aminoalkyl radical and its addition to electron-deficient olefins, thereby revealing the ability of  $\text{B}(\text{C}_6\text{F}_5)_3$  to act as an effective one-electron redox catalyst.<sup>7b,14</sup>

## Result and discussion

At the outset of our study, we selected the commonly used  $\text{B}(\text{C}_6\text{F}_5)_3$  as the Lewis acid because of its ability to oxidize organic molecules<sup>5b-e</sup> and *N*-trimethylsilylmethylaniline derivative **1a** as the Lewis base, considering its low oxidation potential as well as the susceptibility of the corresponding radical cation to irreversibly release a trimethylsilyl cation ( $\text{TMS}^+$ ) to generate an  $\alpha$ -aminomethyl radical.<sup>15</sup> Upon mixing equimolar amounts of **1a** and freshly sublimed  $\text{B}(\text{C}_6\text{F}_5)_3$  in  $\text{CH}_2\text{Cl}_2$  at room temperature, the solution colour immediately changed from colourless to blue green, and the UV-vis absorption spectrum exhibited a local absorption maximum at 648 nm with a broad shoulder (Fig. 1b). This spectrum was in good agreement with that of a mixture of **1a** and  $\text{AgBAr}^f$  ( $\text{BAr}^f = \text{B}(3,5-(\text{CF}_3)_2\text{C}_6\text{H}_3)_4$ ), suggesting that one-electron oxidation of **1a** by  $\text{B}(\text{C}_6\text{F}_5)_3$  had occurred. Electron spin resonance (ESR) experiments allowed the unambiguous assignment of the radical species as **1a**<sup>+</sup> by comparison with the simulated spectrum of one  $^{14}\text{N}$  atom, three  $^1\text{H}$  atoms in the methyl group, two  $^1\text{H}$  atoms in methylene, two  $^1\text{H}$  atoms at the *ortho*-position, two  $^1\text{H}$  atoms at the *meta*-position, and one  $^{29}\text{Si}$  atom with a *g* factor of  $2.0033 > g_e$  (Fig. 1c; see also Table S1 in the ESI† for details of the assignment). The generation of another possible radical, the neutral  $\alpha$ -aminomethyl radical **A**, *via* the release of  $\text{TMS}^+$  from **1a**<sup>+</sup> was limited to an undetectable extent, judging from the comparison with the simulated spectrum of **A**, in which its spin density was localized on a methylene carbon atom (Fig. S6†). The stability of **1a**<sup>+</sup> likely stemmed from the hyper-conjugation effect of the silicon–carbon bond, contributing to the stabilization of the radical cation centre.<sup>15c,g,16</sup>

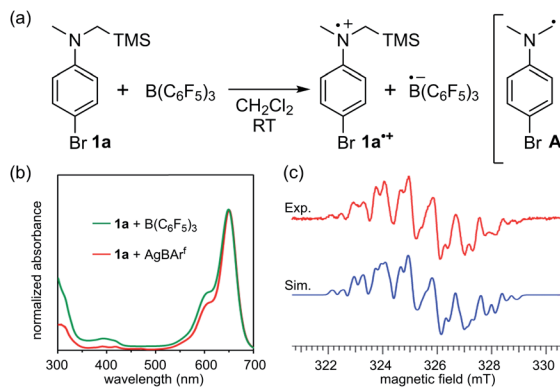


Fig. 1 (a) SET from **1a** to  $\text{B}(\text{C}_6\text{F}_5)_3$ . (b) UV-vis absorption spectra of the mixture of  $\text{B}(\text{C}_6\text{F}_5)_3$  and **1a** (green), and  $\text{AgBAr}^f$  and **1a** (red). (c) Experimentally obtained ESR spectrum of the mixture in  $\text{CH}_2\text{Cl}_2$  (red) and a simulated spectrum of **1a**<sup>+</sup> (blue).

On the basis of the initial observations, we next employed *para*-bromo-*N,N*-dimethylaniline (**2**) as a more common, readily available Lewis base.<sup>17</sup> In this case, an equimolar mixture of  $\text{B}(\text{C}_6\text{F}_5)_3$  and **2** in  $\text{CH}_2\text{Cl}_2$  gave a colourless solution, the ESR analysis of which confirmed that no signal was detected. Intriguingly, however, the solution rapidly turned bright blue green upon irradiation with a 405 nm LED light source. The UV-vis absorption spectrum exhibited a characteristic absorption maximum at 613 nm with a shoulder (Fig. 2b, green), similar to that observed in the spectrum of **1a**<sup>+</sup> (Fig. 1b). This peak was in very good agreement with that of **2**<sup>+</sup> generated separately by the one-electron oxidation of **2** with  $\text{AgSbF}_6$  (Fig. 2b, red). ESR measurements under irradiation provided a well-resolved spectrum of **2**<sup>+</sup>.<sup>18</sup> The eight-fold-integrated spectrum after 1 h of irradiation (Fig. 2c, red) could be assigned to **2**<sup>+</sup>, as it was in good agreement with the simulated spectrum (Fig. 2c, blue) of one  $^{14}\text{N}$  atom, six  $^1\text{H}$  atoms in two methyl groups, two  $^1\text{H}$  atoms at the *ortho*-position, and two  $^1\text{H}$  atoms at the *meta*-position with a *g* factor of  $2.0029 > g_e$  (Table S2†). The saturation of signal intensity after 18 min of irradiation (Fig. 2d) implied a reversible equilibrium for the generation of the radical-ion pair, as illustrated in Fig. 2a. While a signal corresponding to the radical anion  $\text{B}(\text{C}_6\text{F}_5)_3\cdot^-$  was not observed,<sup>5b-e</sup> the rapid attenuation of the signal of **2**<sup>+</sup> upon interruption of irradiation

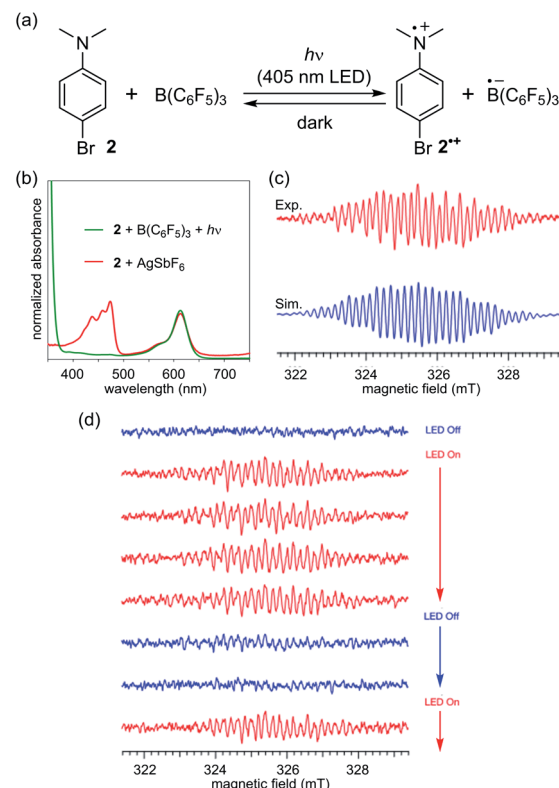


Fig. 2 (a) Photoinduced reversible SET between  $\text{B}(\text{C}_6\text{F}_5)_3$  and **2**. (b) UV-vis spectra of a 1:1 mixture of  $\text{B}(\text{C}_6\text{F}_5)_3$  and **2** after LED light irradiation (green) and  $\text{AgSbF}_6$  and **2** (red). (c) ESR spectrum after 1 h of irradiation with a LED light (red) and a simulated spectrum (blue). (d) LED on/off ESR monitoring experiment of  $\text{B}(\text{C}_6\text{F}_5)_3$  and **2** in  $\text{CH}_2\text{Cl}_2$ . The interval of each measurement is 9 min.



suggested the intervention of a BET process from the pairing radical anion, considering that the ESR signal of  $[2']^+[\text{SbF}_6]^-$  in  $\text{CH}_2\text{Cl}_2$  showed no decay during this time interval (Fig. S7b and  $\dagger$ ). In addition, we confirmed that the signal reappeared immediately upon resuming light irradiation (Fig. 2d).

The outcome of these investigations lead to two important considerations: (1) the origin of the difference in reactivity between **1a** and **2** and (2) the role of the 405 nm light irradiation in the SET to generate a radical-ion pair  $[2']^+[\text{B}(\text{C}_6\text{F}_5)_3]^-$ . The higher reactivity of **1a** can be primarily accounted for by its lower oxidation potential compared to that of **2** (**1a**: 0.23 V, **2**: 0.50 V vs.  $\text{Fc}/\text{Fc}^+$ , Fig. S8 $\dagger$ ), as expected, which originates from the  $\sigma$ -donating effect of the C–Si bond to raise the HOMO level.<sup>16a,c</sup> In addition, the difference in the relative BET rates would be critical. We reasoned that radical cation **1a** $^+$  is stabilized by the  $\beta$ -effect of the silyl group, rendering the BET from the paired  $\text{B}(\text{C}_6\text{F}_5)_3$  $^+$  slower than that in  $[2']^+[\text{B}(\text{C}_6\text{F}_5)_3]^-$ . Owing to the higher energy barrier for SET and the faster BET, external energy (photoirradiation) is essential for **2** to undergo one-electron oxidation by  $\text{B}(\text{C}_6\text{F}_5)_3$  to generate **2** $^+$  in a detectable concentration. This understanding was supported by DFT calculations, which indicated that the difference in the Gibbs free energy between **2** and **2** $^+$  was 4.2 kcal mol $^{-1}$  higher than that between **1a** and **1a** $^+$  (see the ESI $\dagger$  for details of the calculation).

Notwithstanding, no absorption band was detected at approximately 405 nm in the respective absorption spectra of  $\text{B}(\text{C}_6\text{F}_5)_3$  and **2** (Fig. S2 $\dagger$ ), indicating that direct excitation of  $\text{B}(\text{C}_6\text{F}_5)_3$  and **2** is not feasible with 405 nm light. It is important to note, however, that a mixture of  $\text{B}(\text{C}_6\text{F}_5)_3$  and **2** exhibited very weak absorption above 405 nm (Fig. 3a), which suggested a constitutive intermolecular association between  $\text{B}(\text{C}_6\text{F}_5)_3$  and **2**. Fortunately, an orange crystal suitable for X-ray crystallography was obtained from a pentane solution of the mixture cooled to  $-35$  °C in an argon-purged glovebox. Single-crystal X-ray diffraction analysis revealed the three-dimensional structure of a 1 : 1 co-crystal (Fig. 3b), where  $\text{B}(\text{C}_6\text{F}_5)_3$  and **2** were alternately aligned along the  $a$ -axis with face-to-face packing between a  $\text{C}_6\text{F}_5$  moiety of  $\text{B}(\text{C}_6\text{F}_5)_3$  and an aromatic ring of **2** (Fig. 3c). In this association,  $\text{B}(\text{C}_6\text{F}_5)_3$  and **2** were frustrated with the boron centre and the dimethylamino moiety, being oriented opposite to each other, and no Lewis adduct was formed. The average distance between the plane of **2** and the six carbon atoms of the  $\text{C}_6\text{F}_5$  ring that constructs the columnar structure was 3.38 Å, which is close to that of the inner-sphere EDA complex ( $r_{\text{DA}} \approx 3.1 \pm 0.2$  Å).<sup>19</sup> Upon further examining the conformation of  $\text{B}(\text{C}_6\text{F}_5)_3$ , the  $\text{C}_6\text{F}_5$  ring involved in the columnar structure was closer to coplanar with the  $\text{sp}^2$  hybridized boron centre (dihedral angles of C15–B1–C9–C14 and C21–B1–C9–C10 were  $-17.7(6)$ ° and  $-15.0(6)$ °, respectively) compared to the other two  $\text{C}_6\text{F}_5$  rings to effectively achieve the overlap of frontier orbitals with **2** (Fig. 3d, *vide infra* for further discussion). Furthermore, bond alternation was observed in the aniline component of **2**. The N1–C3 bond length was 1.366(6) Å, and the C4–C5 and C7–C8 bond lengths were 1.372(6) and 1.368(6) Å, respectively, which were closer to a carbon–carbon double bond length than to the carbon–carbon bond length of benzene (Table S4 $\dagger$ ). These trends were similar to those

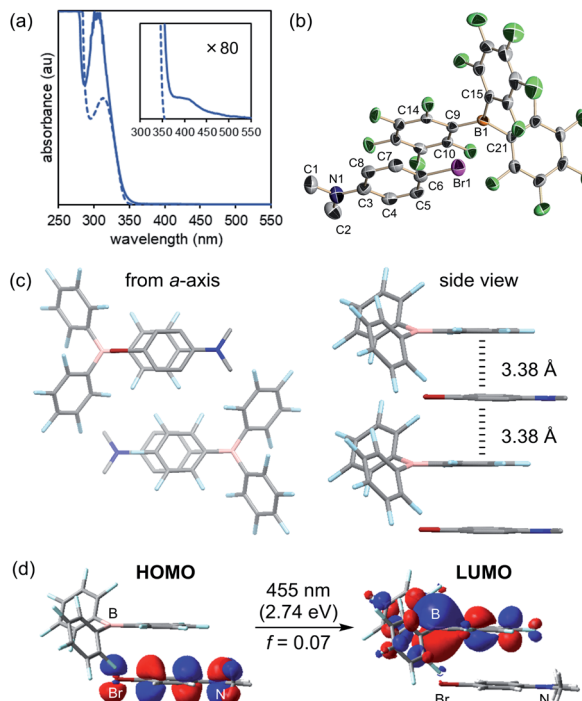
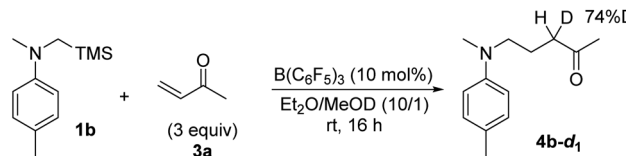


Fig. 3 (a) UV-vis spectra of a 1 : 1 mixture of  $\text{B}(\text{C}_6\text{F}_5)_3$  and **2** (solid line), and **2** (dashed line) for  $1.0 \times 10^{-3}$  M with magnified spectra (inner square). (b) X-ray structure of a co-crystal of  $\text{B}(\text{C}_6\text{F}_5)_3$  and **2**. (c) Packing structure of the co-crystal of  $\text{B}(\text{C}_6\text{F}_5)_3$  and **2**. (d) TD-DFT calculated minimum excitation of the single complex in crystal structure (CAM-B3LYP/6-311+G(d,p)).

reported for the co-crystal of *N,N*-dimethylaniline and electron-deficient hexafluorobenzene,<sup>20</sup> indicating the presence of charge-transfer interactions. To corroborate the charge-transfer characteristics, TD-DFT calculations were conducted for the structure of a single unit of the intermolecular complex in the co-crystal (*anti*-complex). The lowest transition energy of this complex was calculated to be 2.74 eV, corresponding to an absorption at 455 nm, which is consistent with the observation that the crystal was orange in colour and the broad absorption band when present in solution (Fig. 3a). This excitation was assigned to the electronic transition from the HOMO of **2** to the LUMO of  $\text{B}(\text{C}_6\text{F}_5)_3$  (Fig. 3d), and the LUMO, which comprises a  $\pi^*$  orbital of  $\text{C}_6\text{F}_5$  and a  $\text{p}^*$  orbital of boron because of the conformational coplanarity, is effectively overlapped with the HOMO of **2**. This attribute appeared to be independent of the geometry of the complex, as further TD-DFT calculations for the complex with the opposite orientation of **2** (*syn*-complex), where the dimethylamino moiety was located close to the boron centre, indicated analogous absorption (448 nm,  $f = 0.02$ ) and charge-transfer characteristics (Fig. S9 $\dagger$ ). These results suggest that the SET proceeds through the formation of an EDA complex that becomes excited upon 405 nm light irradiation, and that the possibility of a mechanism involving the homolytic cleavage of the B–N coordination bond by photoirradiation is unlikely. This is in accordance with the fact that B–N coordination bond formation between  $\text{B}(\text{C}_6\text{F}_5)_3$  and **2** (Lewis adduct) was not

detected by  $^1\text{H}$  and  $^{11}\text{B}$  NMR spectroscopy, even at  $-90\text{ }^\circ\text{C}$  (Fig. S17 and S18†), and that no absorption at  $405\text{ nm}$  was derived from the TD-DFT calculations for the Lewis adduct (Fig. S13†). These analyses clarified the role of Lewis acid  $\text{B}(\text{C}_6\text{F}_5)_3$  as a  $\pi$ -acceptor and that of Lewis base 2 as a  $\pi$ -donor in this system for photoinduced SET.

Based on these fundamental findings, we envisioned that this unique SET process could potentially be utilized as an elementary step for effecting synthetically relevant transformations. Considering that the radical cations  $\mathbf{1a}^+$  and  $\mathbf{2}^+$  are a precursor of the nucleophilic  $\alpha$ -aminomethyl radical,<sup>15,17</sup> we inferred that they could be trapped by electron-deficient olefins to forge a carbon–carbon bond, providing a basis for further investigation. Thus, an excess amount of methyl vinyl ketone (**3a**) was added as a radical acceptor, initially, to a mixture of **1a** and a catalytic quantity of  $\text{B}(\text{C}_6\text{F}_5)_3$  (10 mol%) in  $\text{CH}_2\text{Cl}_2$ . The expected bond formation indeed occurred and the corresponding radical addition product **4a** was obtained in 31% yield after a standard acidic work-up and purification (Table 1, entry 1). While the use of  $\text{Et}_2\text{O}$  as a solvent led to a slight improvement in chemical yield (entry 2), the efficiency was much affected by the difference in the oxidation potential of **1**, as the reaction of **1b** under similar conditions afforded the product **4b** in 66% yield (**1a**: 0.23 V, **1b**: 0.10 V vs.  $\text{Fc}/\text{Fc}^+$ , Fig. S8†) (entry 3). However, the reactivity was still insufficient and thus, we monitored the reaction in  $\text{THF}-d_8$  by  $^1\text{H}$  NMR spectroscopy to detect possible intermediates.<sup>21</sup> Contrary to our assumption,<sup>15e</sup> a **4b**-derived TMS enol ether was not detected over the course of the reaction, and **4b** was consistently observed before the acidic work-up (Fig. S15†). This profile suggested that a reaction step involving an NMR innocent species was turn-over limiting, and it could be the desilylation from  $\mathbf{1}^+$  that was a major paramagnetic species in the ESR analysis (Fig. 1c). Moreover, after the addition of the resulting  $\alpha$ -aminomethyl radical to **3a**, the transient  $\alpha$ -carbonyl radical would undergo one-electron reduction by  $\text{B}(\text{C}_6\text{F}_5)_3^{\cdot-}$  to form an enolate ion that is



Scheme 1 Deuterium incorporation experiment.

protonated *in situ* by a trace amount of  $\text{H}_2\text{O}$  or **3a**. These considerations and the previous report on the effect of protic solvents for accelerating the desilylation from  $\alpha$ -silyl amine radical cations<sup>15a–c</sup> prompted us to add  $\text{MeOH}$  primarily as a TMS trapping reagent and also as a proton source ( $\text{Et}_2\text{O}/\text{MeOH} = 10/1$ ), which resulted in a dramatic increase in reactivity to afford **4b** in 92% yield even with reduced amounts of **3a** (entry 4). In parallel, the reaction was performed in  $\text{Et}_2\text{O}/\text{MeOD}$  (10/1), giving rise to **4b-d1** in 83% yield with 74% incorporation of deuterium at the internal  $\alpha$ -position of the keto carbonyl group (Scheme 1), and no H–D exchange of isolated **4b** was observed in the presence of  $\text{B}(\text{C}_6\text{F}_5)_3$  and  $\text{MeOD}$  in  $\text{Et}_2\text{O}$  (Scheme S1†). These results strongly support the intermediacy of the enolate ion and its predominant protonation by  $\text{MeOH}$ .

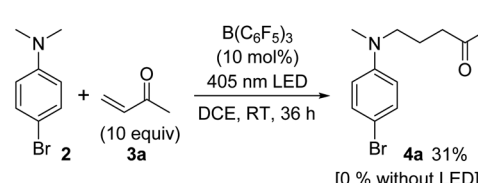
We then moved on to an examination of the reaction between **2** and **3**. In this case, treatment of a mixture of **2** and **3a** with  $\text{B}(\text{C}_6\text{F}_5)_3$  (10 mol%) in 1,2-dichloroethane (DCE) at room temperature for 36 h showed no product formation. However, the reaction irradiated with a 405 nm LED under otherwise identical conditions gave **4a** in 31% yield (Scheme 2). These observations suggested the operation of one-electron redox catalysis of  $\text{B}(\text{C}_6\text{F}_5)_3$  under photoirradiation.

As a more suitable reaction platform for verifying this notion, we selected the coupling of *N*-aryltetrahydroisoquinolines **5** with  $\alpha,\beta$ -unsaturated ketones, which is known to be promoted by a common photoredox catalyst.<sup>22</sup> An initial attempt was made by irradiating a solution of *N*-phenyltetrahydroisoquinoline (**5a**) and **3a** (3.0 equiv.) in DCE under the influence of  $\text{B}(\text{C}_6\text{F}_5)_3$  (10 mol%). This resulted in the formation of the  $\alpha$ -coupling product **6a** in 31% yield (Table S5†), and switching the solvent to acetonitrile (MeCN) delivered an improvement in the chemical yield (70%) (Table 2, entry 1). It should be noted that bond formation did not occur without light irradiation<sup>23</sup> (entry 2), and only a trace amount of **6a** was obtained in the absence of the catalyst (entry 3). In addition, the use of  $\text{BPh}_3$  as a catalyst significantly ruined the reactivity profile (entry 4), and  $\text{BF}_3 \cdot \text{OEt}_2$  was ineffective (entry 5), indicating that the electron-deficient  $\text{C}_6\text{F}_5$  groups are crucial for exerting sufficient catalytic activity. This information bears

Table 1  $\text{B}(\text{C}_6\text{F}_5)_3$ -catalyzed carbon–carbon bond-forming reactions with **1**<sup>a</sup>

Entry	R	Solvent	X	Time (h)	Yield <sup>b</sup> (%)
1	Br ( <b>1a</b> )	$\text{CH}_2\text{Cl}_2$	10	38	31 ( <b>4a</b> )
2	Br ( <b>1a</b> )	$\text{Et}_2\text{O}$	10	38	37 ( <b>4a</b> )
3	Me ( <b>1b</b> )	$\text{Et}_2\text{O}$	10	38	66 ( <b>4b</b> )
4	Me ( <b>1b</b> )	$\text{Et}_2\text{O}/\text{MeOH}$ (10/1)	3	16	92 ( <b>4b</b> )

<sup>a</sup> All reactions were performed in test tubes with septum caps and wrapped with aluminum foil in order to exclude the effect of room light irradiation with 0.1 mmol of **1** and **3a** in a solvent (1 mL) in the presence of 10 mol% of  $\text{B}(\text{C}_6\text{F}_5)_3$  under an Ar atmosphere at room temperature. <sup>b</sup> Isolated yield.



Scheme 2 Trapping experiment of  $\alpha$ -aminomethyl radical generated from **2** with **3a**.



Table 2  $B(C_6F_5)_3$ -catalyzed carbon–carbon bond-forming reactions with 5<sup>a</sup>

Entry	Ar	R <sup>1</sup>	R <sup>2</sup>	Yield <sup>b</sup> (%) (dr)
1	Ph (5a)	H	Me (3a)	70 (6a)
2 <sup>c</sup>	Ph (5a)	H	Me (3a)	0 (6a)
3 <sup>d</sup>	Ph (5a)	H	Me (3a)	<5 (6a)
4 <sup>e</sup>	Ph (5a)	H	Me (3a)	9 (6a)
5 <sup>f</sup>	Ph (5a)	H	Me (3a)	0 (6a)
6	p-MeOC <sub>6</sub> H <sub>4</sub> (5b)	H	Me (3a)	90 (6b)
7	p-BrC <sub>6</sub> H <sub>4</sub> (5c)	H	Me (3a)	61 (6c)
8	o-MeC <sub>6</sub> H <sub>4</sub> (5d)	H	Me (3a)	0 (6d)
9	Ph (5a)	H	Et (3b)	70 (6e)
10	p-MeOC <sub>6</sub> H <sub>4</sub> (5b)	Me	Ph (3c)	76 (1.1 : 1) <sup>g</sup> (6f)

<sup>a</sup> Unless otherwise noted, the reactions were performed with 0.1 mmol of 5 and 0.3 mmol of 3 in MeCN (1 mL) in the presence of 10 mol% of  $B(C_6F_5)_3$  at room temperature under 405 nm LED irradiation under an Ar atmosphere. <sup>b</sup> Isolated yield. <sup>c</sup> No LED irradiation. <sup>d</sup> Without  $B(C_6F_5)_3$ . <sup>e</sup> With  $BPh_3$  instead of  $B(C_6F_5)_3$  as a catalyst. <sup>f</sup> With  $BF_3 \cdot OEt_2$  instead of  $B(C_6F_5)_3$  as a catalyst. <sup>g</sup> Determined by <sup>1</sup>H NMR analysis.

relevance when accounting for the electronic effect of the aryl group attached to the nitrogen atom of 5 on reaction efficiency. When *para*-methoxyphenyl-substituted 5b was employed as a donor component, the coupling product 6b was isolated in a higher yield (90%) (entry 6), whereas the introduction of a *para*-bromophenyl substituent (5c) led to a slight decrease in reactivity (entry 7). The steric demand of the aromatic appendage was also critical, as no evidence of product formation was detected with 5d bearing an *ortho*-tolyl group on the nitrogen (entry 8). These results support the fact that the facile formation of the EDA complex between the N-aryl moiety of 5 and  $B(C_6F_5)_3$  would be essential for the present catalysis. In fact, the formation of EDA complexes with 5a and 5b, but not with 5d, was suggested by UV-vis absorption spectroscopy, and the TD-DFT calculation for the complex of 5a with  $B(C_6F_5)_3$  also supported the charge-transfer characteristics (Fig. S4 and S11,† respectively). With respect to radical acceptors, not only simple vinyl ketones but also other enones, such as phenyl 1-propenyl ketone (3c), were tolerated (entries 9 and 10). On the other hand, less reactive acceptors, such as methyl acrylate and styrene derivatives, were not amenable to this catalytic system. Although we recognize that it is difficult to completely rule out the involvement of a radical-chain process,<sup>22b,24,26,27</sup> the overall nature of this catalysis reflects the oxidation ability of  $B(C_6F_5)_3$  and a redox-neutral catalytic cycle can be operative through the transient generation of radical-ion pairs.

## Conclusions

We have demonstrated the operation of an SET in Lewis pairs between  $B(C_6F_5)_3$  and simple *N,N*-dialkylanilines under dark or

photoirradiation conditions depending on the structure of the aniline derivatives, which was verified by UV-vis and ESR spectroscopic analyses. The key intermediate of this unique SET process was revealed to be an EDA complex involving  $\pi$ -orbital interactions by using absorption spectra, X-ray crystallographic analysis, and DFT calculations. Furthermore, we have shown that these fundamental findings can be exploited for the development of the redox catalysis of  $B(C_6F_5)_3$  for synthetically relevant carbon–carbon bond formation. We anticipate that this study opens a door to a new avenue toward the understanding and exploitation of the reactivity and selectivity of radical-ion pairs generated from Lewis pairs in organic synthesis and catalysis within a single-electron transfer manifold.

## Conflicts of interest

There are no conflicts to declare.

## Acknowledgements

This work is funded by the CREST-JST (JPMJCR13L2: 13418441) and Grants of JSPS for Scientific Research (KAKENHI, 19H00894 and 19K15538). We are grateful to Prof. D. Yokogawa (the University of Tokyo) for his support for computational studies.

## Notes and references

- 1 G. N. Lewis, *Valence and the Structure of Atoms and Molecules*, The Chemical Catalogue Company, New York, 1923.
- 2 H. Yamamoto, *Lewis Acids in Organic Synthesis*, Wiley-VCH, Weinheim, 2000.
- 3 (a) D. W. Stephan and G. Erker, *Angew. Chem., Int. Ed.*, 2010, **49**, 46–76; (b) D. W. Stephan, *J. Am. Chem. Soc.*, 2015, **137**, 10018–10032; (c) D. W. Stephan and G. Erker, *Angew. Chem., Int. Ed.*, 2015, **54**, 6400–6441; (d) A. R. Jupp and D. W. Stephan, *Trends Chem.*, 2019, **1**, 35–48.
- 4 (a) W. F. Forbes, P. D. Sullivan and H. M. Wang, *J. Am. Chem. Soc.*, 1967, **89**, 2705–2711; (b) H. van Willigen, *J. Am. Chem. Soc.*, 1967, **89**, 2229–2230; (c) F. A. Bell, A. Ledwith and D. C. Sherrington, *J. Chem. Soc. C*, 1969, 2719–2720; (d) W. Schmidt and E. Steckhan, *Chem. Ber.*, 1980, **113**, 577–585; (e) S. Dapperheld, E. Steckhan, K.-H. G. Brinkhaus and T. Esch, *Chem. Ber.*, 1991, **124**, 2557–2567; (f) C. J. Harlan, T. Hascall, E. Fujita and J. R. Norton, *J. Am. Chem. Soc.*, 1999, **121**, 7274–7275.
- 5 (a) G. Ménard, J. A. Hatnean, H. J. Cowley, A. J. Lough, J. M. Rawson and D. W. Stephan, *J. Am. Chem. Soc.*, 2013, **135**, 6446–6449; (b) X. Zheng, X. Wang, Y. Qiu, Y. Li, C. Zhou, Y. Sui, Y. Li, J. Ma and X. Wang, *J. Am. Chem. Soc.*, 2013, **135**, 14912–14915; (c) L. Liu, L. L. Cao, Y. Shao, G. Ménard and D. W. Stephan, *Chem.*, 2017, **3**, 259–267; (d) Z. Dong, H. H. Cramer, M. Schmidtmann, L. A. Paul, I. Siewert and T. Müller, *J. Am. Chem. Soc.*, 2018, **140**, 15419–15424; (e) L. L. Liu, L. L. Cao, D. Zhu, J. Zhou and D. W. Stephan, *Chem. Commun.*, 2018, **54**, 7431–7434; (f) A. Merk, H. Großkappenberg, M. Schmidtmann, M.-P. Luecke, C. Lorent, M. Driess, M. Oestreich,



H. F. T. Klare and T. Müller, *Angew. Chem., Int. Ed.*, 2018, **57**, 15267–15271; (g) Y. Kim, L. L. Liu and D. W. Stephan, *Chem.–Eur. J.*, 2019, **25**, 7110–7113; (h) L. L. Liu and D. W. Stephan, *Chem. Soc. Rev.*, 2019, **48**, 3454–3463.

6 During the preparation of this manuscript, an elegant work on the application of SET in  $\text{PMes}_3$  and  $\text{B}(\text{C}_6\text{F}_5)_3$  to C–C bond-forming reaction with a stoichiometric amount of the Lewis pair was reported. Y. Soltani, A. Dasgupta, T. A. Gazis, D. M. C. Ould, E. Richards, B. Slater, K. Stefkova, V. Y. Vladimirov, L. C. Wilkins, D. Willcox and R. L. Melen, *Cell Reports Physical Science*, 2020, **1**, 100016.

7 (a) R. S. Mulliken, *J. Am. Chem. Soc.*, 1952, **74**, 811–824; (b) C. G. S. Lima, T. d. M. Lima, M. Duarte, I. D. Jurberg and M. W. Paixão, *ACS Catal.*, 2016, **6**, 1389–1407.

8 A. V. Vasilyev, S. V. Lindeman and J. K. Kochi, *New J. Chem.*, 2002, **26**, 582–592.

9 U. M. Rabie, *J. Mol. Struct.*, 2013, **1034**, 393–403.

10 (a) E. K. Kim and J. K. Kochi, *J. Am. Chem. Soc.*, 1991, **113**, 4962–4974; (b) S. V. Rosokha and J. K. Kochi, *J. Am. Chem. Soc.*, 2001, **123**, 8985–8999.

11 (a) T. Dohi, M. Ito, N. Yamaoka, K. Morimoto, H. Fujioka and Y. Kita, *Angew. Chem., Int. Ed.*, 2010, **49**, 3334–3337; (b) N. Yamaoka, K. Sumida, I. Itani, H. Kubo, Y. Ohnishi, S. Sekiguchi, T. Dohi and Y. Kita, *Chem.–Eur. J.*, 2013, **19**, 15004–15011; (c) H. Jiang, Y. He, Y. Cheng and S. Yu, *Org. Lett.*, 2017, **19**, 1240–1243; (d) H.-Y. Tu, S. Zhu, F.-L. Qing and L. Chu, *Chem. Commun.*, 2018, **54**, 12710–12713.

12 (a) S. C. Blackstock, J. P. Lorand and J. K. Kochi, *J. Org. Chem.*, 1987, **52**, 1451–1460; (b) Y. Cheng, X. Yuan, J. Ma and S. Yu, *Chem.–Eur. J.*, 2015, **21**, 8355–8359.

13 (a) T. A. Rokob, A. Hamza, A. Stirling, T. Soós and I. Pápai, *Angew. Chem., Int. Ed.*, 2008, **47**, 2435–2438; (b) T. A. Rokob, A. Hamza, A. Stirling and I. Pápai, *J. Am. Chem. Soc.*, 2009, **131**, 2029–2036; (c) S. Grimme, H. Kruse, L. Goerigk and G. Erker, *Angew. Chem., Int. Ed.*, 2010, **49**, 1402–1405; (d) M. Pu and T. Privalov, *J. Chem. Phys.*, 2013, **138**, 154305; (e) L. Rocchigiani, G. Ciancaleoni, C. Zuccaccia and A. Macchioni, *J. Am. Chem. Soc.*, 2014, **136**, 112–115.

14 For seminal contributions to the exploitation of EDA-complex formation in controlling catalytic bond formations, see: (a) E. Arceo, I. D. Jurberg, A. Álvarez-Fernández and P. Melchiorre, *Nat. Chem.*, 2013, **5**, 750–756; (b) A. Bahamonde and P. Melchiorre, *J. Am. Chem. Soc.*, 2016, **138**, 8019–8030; (c) Z.-Y. Cao, T. Ghosh and P. Melchiorre, *Nat. Commun.*, 2018, **9**, 3274. For recent examples of catalysis *via* EDA-complex formation, see: (d) R. P. Shirk and S. S. V. Ramasastry, *Org. Lett.*, 2017, **19**, 5482–5485; (e) I. Bosque and T. Bach, *ACS Catal.*, 2019, **9**, 9103–9109.

15 (a) U. C. Yoon, J. U. Kim, E. Hasegawa and P. S. Mariano, *J. Am. Chem. Soc.*, 1987, **109**, 4421–4423; (b) E. Hasegawa, W. Xu, P. S. Mariano, U. C. Yoon and J. U. Kim, *J. Am. Chem. Soc.*, 1988, **110**, 8099–8111; (c) U. C. Yoon and P. S. Mariano, *Acc. Chem. Res.*, 1992, **25**, 233–240; (d) D. W. Cho, U. C. Yoon and P. S. Mariano, *Acc. Chem. Res.*, 2011, **44**, 204–215; (e) Y. Miyake, Y. Ashida, K. Nakajima

and Y. Nishibayashi, *Chem. Commun.*, 2012, **48**, 6966–6968; (f) Y. Miyake, Y. Ashida, K. Nakajima and Y. Nishibayashi, *Chem.–Eur. J.*, 2014, **20**, 6120–6125; (g) K. Nakajima, M. Kitagawa, Y. Ashida, Y. Miyake and Y. Nishibayashi, *Chem. Commun.*, 2014, **50**, 8900–8903; (h) D. Lenhart and T. Bach, *Beilstein J. Org. Chem.*, 2014, **10**, 890–896; (i) L. Ruiz Espelt, I. S. McPherson, E. M. Wiensch and T. P. Yoon, *J. Am. Chem. Soc.*, 2015, **137**, 2452–2455; (j) K. Nakajima, Y. Ashida, S. Nojima and Y. Nishibayashi, *Chem. Lett.*, 2015, **44**, 545–547; (k) C. Wang, Y. Zheng, H. Huo, P. Röse, L. Zhang, K. Harms, G. Hilt and E. Meggers, *Chem.–Eur. J.*, 2015, **21**, 7355–7359; (l) D. Lenhart, A. Bauer, A. Pöthig and T. Bach, *Chem.–Eur. J.*, 2016, **22**, 6519–6523; (m) S.-Y. Hsieh and J. W. Bode, *Org. Lett.*, 2016, **18**, 2098–2101; (n) T. Kizu, D. Uraguchi and T. Ooi, *J. Org. Chem.*, 2016, **81**, 6953–6958; (o) W. Ding, L.-Q. Lu, J. Liu, D. Liu, H.-T. Song and W.-J. Xiao, *J. Org. Chem.*, 2016, **81**, 7237–7243; (p) Y. Zhao, J.-R. Chen and W.-J. Xiao, *Org. Lett.*, 2016, **18**, 6304–6307; (q) C. Remeur, C. B. Kelly, N. R. Patel and G. A. Molander, *ACS Catal.*, 2017, **7**, 6065–6069; (r) X. Shen, Y. Li, Z. Wen, S. Cao, X. Hou and L. Gong, *Chem. Sci.*, 2018, **9**, 4562–4568; (s) Y. Cai, Y. Tang, L. Fan, Q. Lefebvre, H. Hou and M. Rueping, *ACS Catal.*, 2018, **8**, 9471–9476; (t) A. Casado-Sánchez, P. Domingo-Legarda, S. Cabrera and J. Alemán, *Chem. Commun.*, 2019, **55**, 11303–11306; (u) M. Grübel, C. Jandl and T. Bach, *Synlett*, 2019, **30**, 1825–1829.

16 (a) B. E. Cooper and W. J. Owen, *J. Organomet. Chem.*, 1971, **29**, 33–40; (b) H. Bock and W. Kaim, *Acc. Chem. Res.*, 1982, **15**, 9–17; (c) J. Yoshida, T. Maekawa, T. Murata, S. Matsunaga and S. Isoe, *J. Am. Chem. Soc.*, 1990, **112**, 1962–1970.

17 (a) A. McNally, C. K. Prier and D. W. C. MacMillan, *Science*, 2011, **334**, 1114–1117; (b) Y. Miyake, K. Nakajima and Y. Nishibayashi, *J. Am. Chem. Soc.*, 2012, **134**, 3338–3341; (c) H. Zhou, P. Lu, X. Gu and P. Li, *Org. Lett.*, 2013, **15**, 5646–5649; (d) C. Zhang, C. Liu, Y. Shao, X. Bao and X. Wan, *Chem.–Eur. J.*, 2013, **19**, 17917–17925; (e) C. K. Prier and D. W. C. MacMillan, *Chem. Sci.*, 2014, **5**, 4173–4178; (f) A. Noble and D. W. C. MacMillan, *J. Am. Chem. Soc.*, 2014, **136**, 11602–11605; (g) X. Dai, D. Cheng, B. Guan, W. Mao, X. Xu and X. Li, *J. Org. Chem.*, 2014, **79**, 7212–7219; (h) X. Dai, R. Mao, B. Guan, X. Xu and X. Li, *RSC Adv.*, 2015, **5**, 55290–55294; (i) D. Uraguchi, N. Kinoshita, T. Kizu and T. Ooi, *J. Am. Chem. Soc.*, 2015, **137**, 13768–13771; (j) K. Nakajima, Y. Miyake and Y. Nishibayashi, *Acc. Chem. Res.*, 2016, **49**, 1946–1956; (k) H. B. Hepburn and P. Melchiorre, *Chem. Commun.*, 2016, **52**, 3520–3523; (l) J. J. Murphy, D. Bastida, S. Paria, M. Fagnoni and P. Melchiorre, *Nature*, 2016, **532**, 218; (m) C. Wang, J. Qin, X. Shen, R. Riedel, K. Harms and E. Meggers, *Angew. Chem., Int. Ed.*, 2016, **55**, 685–688; (n) E. Fava, A. Millet, M. Nakajima, S. Loescher and M. Rueping, *Angew. Chem., Int. Ed.*, 2016, **55**, 6776–6779; (o) L. Li, T. Xiao, H. Chen and L. Zhou, *Chem.–Eur. J.*, 2017, **23**, 2249–2254; (p) C.-W. Hsu and H. Sundén, *Org. Lett.*, 2018, **20**, 2051–2054.



18 The generation of paramagnetic species in the solution of  $B(C_6F_5)_3$  and *N,N*-dimethylaniline was described in W. E. Piers, *Adv. Organomet. Chem.*, 2005, **52**, 1–76; however, the precise analysis of the paramagnetic species has not been achieved.

19 S. V. Rosokha and J. K. Kochi, *Acc. Chem. Res.*, 2008, **41**, 641–653.

20 T. Dahl, *Acta Crystallogr., Sect. C: Cryst. Struct. Commun.*, 1985, **41**, 931–933.

21 Compound **4b** was obtained in 57% yield with 10 equivalents of **3a** when THF was used as solvent.

22 (a) P. Kohls, D. Jadhav, G. Pandey and O. Reiser, *Org. Lett.*, 2012, **14**, 672–675; (b) L. Ruiz Espelt, E. M. Wiensch and T. P. Yoon, *J. Org. Chem.*, 2013, **78**, 4107–4114; (c) J. Xuan, T.-T. Zeng, Z.-J. Feng, Q.-H. Deng, J.-R. Chen, L.-Q. Lu, W.-J. Xiao and H. Alper, *Angew. Chem., Int. Ed.*, 2015, **54**, 1625–1628; (d) S.-X. Lin, G.-J. Sun and Q. Kang, *Chem. Commun.*, 2017, **53**, 7665–7668; (e) J. Zheng and B. Breit, *Angew. Chem., Int. Ed.*, 2019, **58**, 3392–3397.

23 Performing the reaction with the light irradiation at fixed intervals under otherwise identical conditions revealed that the bond formation proceeded only when irradiated (Fig. S14†).

24 We tried to determine the quantum yield of the reaction reported in entry 1, Table 2 by the standard ferrioxalate actinometry according to the literature procedure.<sup>25</sup> However, the reaction did not proceed within the range of the photon flux density that could be determined by the method, which might suggest a low quantum yield value.

25 (a) C. G. Hatchard and C. A. Parker, *Proc. R. Soc. London, Ser. A*, 1956, **235**, 518–536; (b) M. A. Cismesia and T. P. Yoon, *Chem. Sci.*, 2015, **6**, 5426–5434; (c) C. B. Tripathi, T. Ohtani, M. T. Corbett and T. Ooi, *Chem. Sci.*, 2017, **8**, 5622–5627.

26 (a) R. Mosca, M. Fagnoni, M. Mella and A. Albini, *Tetrahedron*, 2001, **57**, 10319–10328; (b) N. Hoffmann, S. Bertrand, S. Marinković and J. Pesch, *Pure Appl. Chem.*, 2006, **78**, 2227–2246.

27 We conducted crossover experiments with **1b** and excess amount of **2** or **5a** using **3a** as an acceptor and  $B(C_6F_5)_3$  as a catalyst (10 mol%) under dark conditions (see Scheme S2† for details). In both cases, the formation of crossover product **4a** or **6a** was not detected, and **4b** was obtained as a sole product. These results suggest that the intervention of the radical-chain process is marginal.

